Static and dynamic critical behavior of a binary polymer blend in the strong fluctuation limit: A light scattering study

W. Theobald and G. Meier*
Max-Planck-Institut für Polymerforschung, Postfach 3148, 55021 Mainz, Germany
(Received 31 October 1994)

Based upon previous work [G. Meier, B. Momper, and E. W. Fischer, J. Chem. Phys. **97**, 5884 (1992)], we report light scattering experiments of the binary polymer blend poly (dimethylsiloxane), PDMS ($N=225$), and poly (ethylmethylsiloxane), PEMS ($N=325$), with N being the degree of polymerization at the critical composition $\phi_{c,\mathrm{PEMS}}=0.456$ in the temperature range $8\times10^{-4}<\varepsilon<4\times10^{-2}$, with $\varepsilon=T-T_c/T$ being the reduced temperature. Using an Ornstein-Zernike scattering law we extract the static structure factor $S(\mathbf{q}=\mathbf{0})$ from the angular dependence of the scattered intensity thereby taking the correction for turbidity into account which has become necessary due to the proximity to T_c in contrast to the previous study. From an analysis of $S(\mathbf{q}=\mathbf{0})$ with a crossover function describing the change from mean field to three-dimensional Ising behavior close to the critical point, we calculate the Ginzburg number Gi which now quantitatively allows us to identify the Ising regime for $\varepsilon<$ Gi. In this region, the strong fluctuation limit, we obtain the critical exponents $\gamma=1.24\pm0.02$, $\nu=0.62\pm0.01$, and $\eta=0.036\pm0.002$ in agreement with values from renormalization group calculations for the three-dimensional Ising universality class. From the angular dependence of the Rayleigh linewidth we obtain the critical exponent x_η which determines the divergence of the viscosity while approaching the critical point to be $x_\eta=0.06\pm0.03$ in agreement with theory. We further establish the crossover of the relaxation rate Γ in the mode coupled regime ($\xi>R_gN^{1/2}$) from $\Gamma\propto\varepsilon^{\nu}$ for $q\xi<1$ to $\Gamma\propto\varepsilon^{\nu x_\eta}$ for $q\xi>1$ thereby considering the weak divergence of the viscosity. The proposed crossover of Γ from $\Gamma\propto q^4\varepsilon^{\nu x_\eta}$ (non-mode coupled) for $qR_g<N^{-1/2}$ to $\Gamma\propto q^3\varepsilon^{\nu x_\eta}$ (mode coupled) for $qR_g>N^{-1/2}$ was not observed due to the small background contribution. We conclude that a polymer mixture where viscoelastic effects are small behaves for $\varepsilon<$ Gi exactly like a simple ordinary binary liquid belonging to the model H of Hohenberg and Halperin. Anomalies in the viscosity exponent x_η, as has been reported for polymer-solvent systems [Phys. Rev. B **12**, 368 (1975)], were not detected.

PACS number(s): 05.70.Jk, 36.20.−r, 64.60.Fr, 78.47.+p

I. INTRODUCTION

The static properties of critical polymer blends in the one phase region have already been investigated by small-angle x-ray scattering [1,2], synchrotron radiation [3], and mainly by small-angle neutron scattering [4–16]. Light scattering experiments have been employed further to study dynamical critical behavior. However, there are only two studies [17,18] dealing with this topic so far opening a rich new field. In all cited references it was found that polymer blends may be treated as mean field systems using the random phase approximation (RPA) developed in this case by de Gennes [19] if the molecular weights of the constituents are high and the distance from the critical point is large. However, close to the second order phase transition, a crossover to the three-dimensional Ising behavior occurs, which has been manifested by a large variety of experiments [9,10,13–18]. Recently, it was further made possible to describe this crossover quantitatively [20,21] on the basis of a crossover function proposed by Kiselev and co-workers [22,23]. From such an analysis the Ginzburg number Gi, which is a measure of the magnitude of the fluctuations in the system, can be deduced which separates the mean field region from the Ising regime. Based upon our previous work [18] of a poly (dimethylsiloxane)-poly(ethylmethylsiloxane) (PDMS-PEMS) blend, we intend in this study of the same system (however, here the total N differs, being 10% less) to concentrate only on the Ising regime, both in the static and dynamic properties of the system. In that region where ξ, the correlation length of order parameter fluctuations, is expected to be in the order of $\xi>R_gN^{1/2}$, (where R_g is the radius of gyration of the polymer coil), the polymeric nature of the system is lost since the only relevant length is ξ, which largely exceeds structural aspects. So one may naively argue that such a system may be treated as a simple binary liquid. Then, consequently, this restriction to the Ising regime (where mode-coupling occurs) in a wide sense releases us from using arguments based upon the RPA. Naturally, we try to avoid items, such as the Flory-Huggins χ parameter or mean field critical temperature, since they seem to be unsuitable to describe the physics for $\varepsilon\ll$ Gi. This treatment is along the line already opened up in Refs. [20 and 24] and was further supported by Binder by

*Corresponding author.

Monte Carlo simulations [25]. However, we intend to avoid the RPA more rigorously.

Despite the fact that we observe Ising-like behavior for $\varepsilon < \mathrm{Gi}$, the scattering pattern may be described by an Ornstein-Zernike law [26,27]. Distinct deviations are marked for $q\xi \gg 1$, which we do not reach in our experiments.

Furthermore, it is interesting to compare our viscosity scaling results with those recently obtained from a polymer-solvent system [28]. This is considered to behave also like the Ising regime. Here considerable deviations from the divergence of the viscosity have been found [29]. On the basis of this viscosity correction, our results may be further compared with recent data by Miyashita and Nose [30] also on a polymer-solvent system. They have found deviations from the modified Kawasaki scaling function. It seems to be important to find out whether polymer blend systems in the strong fluctuation limit behave differently than polymer-solvent systems that also fall into the Ising universality class.

In this context, the discussion raised by Tanaka [31] seems to be notable, because he doubts that polymer systems belong to the same universality class as classical fluids, namely, the so-called model H of Hohenberg and Halperin [32]. What governs that is a proposed kinetic coupling between the stress field ($\sim$ viscoelasticity) and the order parameter. We shall try to address this point in the last section.

Finally, Binder has argued [33] that the crossover between the mean field and Ising should occur in the same region as the crossover between nonmode coupled and mode coupled dynamics, a fact that was confused in earlier experimental [17,18] and theoretical studies [34]. We shall try to give experimental evidence that this conjecture seems to be correct on the basis of our data.

The paper is organized in the following way: Sec. II A is a theoretical reminder concerning the static properties on the basis of the space correlation function of order parameter fluctuations. Section II B deals with the dynamic aspects especially with the viscosity divergence, the scaling function, the identification of various regimes depending on whether $q\xi$ is larger or smaller than 1 and (qR_g^{-1}) is larger or smaller than $\sqrt{N}$ and the crossover between these. Section III A is the experimental part followed by III B describing the data treatment including the turbidity correction. Then in Sec. IV the results of the static properties and in Sec. V the results of the dynamic properties are presented. We discuss and conclude with Sec. VI.

II. THEORETICAL REMINDER

In this section, we give a short survey of the underlying theoretical formalisms needed to discuss the issue further. In the static part we basically refer to the book by Binney *et al.* [35], whereas the dynamical aspects are illuminated by Fredrickson [34] and further on reformulated and corrected by Binder [33].

A. Statics

We start our reminder by considering the two point order parameter [36] correlation function $G^{(2)}(\mathbf{r})$. It measures the correlation between the concentration at two points $\mathbf{r}_1$ and $\mathbf{r}_2$,

$$G_{AB}^{(2)}(\mathbf{r}_1-\mathbf{r}_2) := G^{(2)}(\mathbf{r}) = \langle \phi_A(\mathbf{r}_1)\phi_B(\mathbf{r}_2)\rangle - \langle \phi_A\rangle\langle \phi_B\rangle \ , \tag{2.1}$$

where A and B are the polymer species. There is only one independent correlation function in the system $G_{AA}^{(2)} = G_{BB}^{(2)} = -G_{AB}^{(2)} = G^{(2)}$. The interesting question now is, what is the form of $G^{(2)}$ close to and at T_c? At T_c, one finds an asymptotic form for large r compared with intermolecular distances

$$G^{(2)}(\mathbf{r}) \propto \frac{1}{r^{d-2+\eta}} \quad (r \text{ large}, T = T_c) \ . \tag{2.2}$$

Here d is the dimensionality ($d=3$) and η is a critical exponent that basically describes the decay of correlations at T_c. For $T \neq T_c$, $G^{(2)}(\mathbf{r})$ cannot be described by a simple power law, but,

$$G^2(\mathbf{r}) \propto \frac{1}{r^{d-2}} f\left[\frac{r}{\xi}\right] \quad (r \text{ large}, \ T \neq T_c) \ . \tag{2.3}$$

However, it was found to be approximately correct to write, if $q\xi$ is not too large [26], for $G^{(2)}(\mathbf{r})$ an Ornstein-Zernike (OZ) form. In Eq. (2.3) a new length, the correlation length ξ, is introduced. The order parameter fluctuates in blocks of all sizes up to size ξ, but fluctuations that are significantly larger than ξ are rare. The temperature variation of ξ is given by

$$\xi = \xi_0 \varepsilon^{-\nu} \ , \tag{2.4}$$

where ν is the critical exponent of the correlation length and $\varepsilon = (T - T_c)/T$ is the reduced temperature. We would like to add a note on how the reduced temperature is defined here. Usually $\varepsilon = (T - T_c)/T$ for polymeric systems, because the Flory-Huggins χ parameter has a $\chi \propto T^{-1}$ dependence [8]. By that this definition of ε differs from the usual one used in the physics of critical phenomena [37] $[(T - T_c)/T_c]$. However, as one can easily calculate, in the region of $T - T_c$ we encounter here for $\varepsilon < \mathrm{Gi}$, no matter how ε is defined, the difference between $\ln[(T - T_c)/T]$ and $\ln[(T - T_c)/T_c]$ is small within the third decimal after the dot, hence inconsequential.

The experimentally accessible quantity is the Fourier transformation of Eq. (2.1), the static structure factor $S(\mathbf{q})$,

$$S(\mathbf{q}) = \frac{1}{a^3} \int d^3\mathbf{r} \exp i\mathbf{q}\cdot\mathbf{r} G(\mathbf{r}) \ , \tag{2.5}$$

where the factor a^{-3} is introduced to make $S(\mathbf{q})$ dimensionless. From $S(\mathbf{q})$, the susceptibility $S(\mathbf{q}=0)$ is easily obtained (i.e., by an Ornstein-Zernike plot [18]). $S(\mathbf{q}=\mathbf{0}) := S(\mathbf{0})$ shows a divergence as the system approaches the critical point, since at $T = T_c$, $S^{-1}(\mathbf{0}) = (1/kT)(\partial^2 F/\partial\phi^2) = 0$ where F is the free energy of the system. The temperature variation of $S(\mathbf{0})$ is given

TABLE I. Values of the critical exponents ν, γ, and η from renormalization group calculations for the three-dimensional Ising case [38] and comparison with experiment (this study).

	Theory	Experiment
ν	0.6310±0.0015	0.62±0.01
γ	1.2390±0.0025	1.24±0.02
η	0.0375±0.0025	0.036±0.002

by

$$S(\mathbf{0})=S_0\varepsilon^{-\gamma}\,, \tag{2.6}$$

where γ is the critical exponent of the susceptibility. If one solves Eq. (2.5) explicitly for the $G(\mathbf{r})$, as given by Eq. (2.3) then the well-known OZ scattering law results in

$$S(\mathbf{q})=S(\mathbf{0})(1+q^2\xi^2)^{-1} \tag{2.7}$$

which we may also write $S(q)\propto(1/q^2+\xi^{-2})$. Now we see easily that for $T\to T_c$, $\xi\to\infty$ yielding $S(q)\propto q^{-2}$ being the OZ scaling. On the other hand, the Fourier transform using Eq. (2.2) gives $S(q)\propto q^{\eta-2}$, which is a correction to scaling. On the basis of this result we may accordingly write in summary

$$S(\mathbf{q})=A\varepsilon^{-\gamma}g(q\xi)\,, \tag{2.8}$$

where $g(q\xi)^{-1}=1+q^2\xi^2$ for all practical cases here and A is an amplitude that is defined when $\lim_{x\to 0}g(x)=1$.

The critical exponents η, ν, and γ appearing in Eqs. (2.2), (2.4), and (2.6), respectively, as obtained from theoretical calculations are listed in Table I and compared with the experimentally obtained results from this study.

B. Dynamics

The central quasielastic component in the spectrum of scattered light is caused by the diffusive decay of concentration fluctuations. Its decay rate $\Gamma(\mathbf{q})$ is given by [39]

$$\Gamma(\mathbf{q})=\frac{\Lambda(\mathbf{q})}{S(\mathbf{q})}q^2\,, \tag{2.9}$$

where $\Lambda(\mathbf{q})$ is the Onsager coefficient and $S(\mathbf{q})$ is the susceptibility of the system, diverging for $T\to T_c$. Note that after inserting an OZ ansatz [Eq. (2.7)] for $S(\mathbf{q})$, the critical slowing down (Γ goes to zero) of the system should scale with

$$\Gamma(\mathbf{q})=Bq^2(1+q^2\xi^2)\propto O(q^4)\,, \tag{2.10}$$

where the constant B may be expressed in terms of the Rouse theory in our case [18,33]. The general form of Eq. (2.9) remains valid even in the vicinity of the critical point, however, then the Onsager coefficient has to be renormalized due to mode coupling effects [40,41]. This stems from the fact that there long range order parameter fluctuations occur that are transmitted by velocity fluctuations. Generally, one can show theoretically that for $qR_g\ll 1$ the decay rate including mode coupling corrections for polymer blends is given by [34]

$$\Gamma(\mathbf{q})=\frac{kT}{6\pi\eta_s}\frac{S(\mathbf{0})}{S(\mathbf{q})}[\xi^{-1}F(q\xi)+CR_gN^{1/2}\xi^{-2}]q^2 \tag{2.11}$$

with $F(x)=\frac{3}{4}[(x^{-1}-x^{-3})\arctan x+x^{-2}]$ being Ferrell's scaling function [39], C being a constant in the order of unity, and η_s being the macroscopic shear viscosity.

Now, the following cases may be discussed [33].

For $qR_g\gg N^{-1/2}$ the form of Eq. (2.10) is recovered and hence mode coupling corrections are unimportant. However, for $q\xi\gg 1$ (strong fluctuation limit) and $qRg\ll N^{-1/2}$ one gets $\Gamma(q)\propto(q\xi)^3$. In this, polymer mixtures act like ordinary mixtures with respect to the scaling behavior. Experimentally, the predicted dependence of the decay rate $\propto q^3$ for $\varepsilon\ll 1$ in contrast to the hydrodynamics case $\propto q^2$ for $\varepsilon\gg 1$ has already been observed [17,18]. The cases in the limit $q\xi\ll 1$, which we are not dealing with in this study, are further discussed by Binder [33]. Furthermore, Binder theoretically showed that the static crossover between mean field to Ising behavior occurs in the same regime as the crossover from mode coupled to nonmode coupled dynamics. Figure 1 displays all relevant findings schematically: The main differences between Fig. 1 and the corresponding diagrams in Refs. [17] and [18] based on Fredricksons work [34] is twofold: First, there is experimentally no crossover between mean field to Ising at $\xi=R_g$, as was erroneously stated by Stepanek *et al.* [17], if the crossover is properly analyzed using a crossover function [20]. However, at $\xi=R_g$ another physical phenomena takes place, namely the localization of individual coils which occurs when the

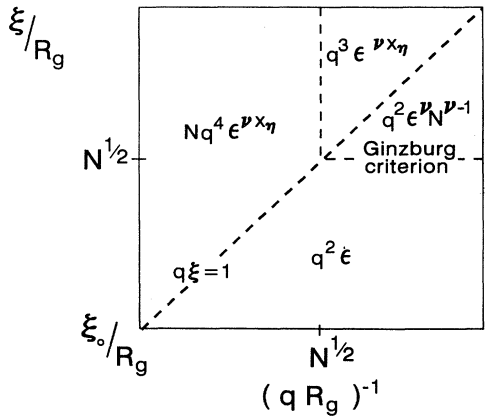

FIG. 1. Schematic illustration of the various regimes for the reduced relaxation rate $\Gamma^*=(\eta/kT)\Gamma(\mathbf{q})$ in different regimes of wavelength q^{-1} and correlation length ξ after Binder [33]. In this study we concentrate only on the upper right part of the diagram for $qR_g>N^{-1/2}$ thereby varying $q\xi$ larger or smaller than 1 and furthermore for $\xi/R_g>N^{1/2}$ varying (qR_g) larger or smaller than $N^{-1/2}$. Note, that throughout $\varepsilon^{\nu x_\eta}=\varepsilon^{+0.004}$ is written instead of ε^0, which results from taking the divergence of η_s into account, which is not the case in Ref. [34]. The Ginzburg criterion was confirmed using a crossover function (see Sec. IV).

effective potential, which is the Fourier transform of the Hamiltonian describing the effective monomer-monomer potential, changes sign [42]. Further consequences of this effect are not considered in this paper. However, the importance of it with respect to conformational properties of the blend under study (which are not important for $\varepsilon \ll 1 < \mathrm{Gi}$) have been thoroughly analyzed and will be published elsewhere [43].

Second, there is no mode coupling in the mean field regime which results basically from the proper analysis of the Ginzburg criterion. The previously experimentally found crossover [18] from ε^{ν} to $\varepsilon^{2\nu}$ for $\xi < 0.1 N^{1/2} R_g$ is not in agreement with Binder's result [33]. However, the experimental fact still remains what causes deviations from the ε^{ν} regime at large distances from T_c? Since here we are only interested in the limit of strong fluctuations this point is not discussed further.

In summary, we may observe dynamic crossover between $q^2\varepsilon^{\nu}$ to $q^3\varepsilon^{\nu x_\eta}$ at constant $(qR_g)^{-1}$ and furthermore at constant ξ/R_g the crossover between $q^4\varepsilon^{\nu x_\eta}$ to $q^3\varepsilon^{\nu x_\eta}$, possibly for low q data.

However, in the derivations so far [33,34], the weak divergence of the viscosity has been neglected. It is taken into account by

$$\eta_s = \eta_0 (q_0 \xi)^{x_\eta} , \tag{2.12}$$

where q_0 is a system dependent amplitude that is related to the background and the Debye cutoff [18,44]. η_0 is the bare viscosity coefficient and the critical exponent x_η has the value $x_\eta = 0.065$ [45]. It can be obtained [44] from the angular dependence of the Rayleigh linewidth $\Gamma(\mathbf{q}) \propto q^{z_{\mathrm{eff}}}$. Then by extrapolation linearily to T_c we obtain as the limiting value

$$z = \lim_{T \to T_c} z_{\mathrm{eff}} = 3 + x_\eta . \tag{2.13}$$

Hence, in all equations appearing within the mode coupled regime showing a ε^0 term (Fig. 4 in Ref. [33]) we have to substitute according to $\Gamma(\mathbf{q}) \propto \eta_s^{-1} \propto \xi^{-x_\eta} \propto \varepsilon^{x_\eta \nu} = \varepsilon^{0.041}$. Then the basic equation for the reduced linewidth Γ^* [cf. Eq. (2.11)]

$$\Gamma^* = \frac{6\pi\eta_s}{kT} \frac{\Gamma(\mathbf{q})}{q^3} \tag{2.14}$$

is given by the scaling function derived by Burstyn *et al.* [46]

$$\Gamma^* = \frac{R}{x} K(x) (1 + b^2 x^2)^{x_\eta/2} \tag{2.15}$$

with $R = 1.027$, $b = 0.55$, $x = q\xi$, and $K(x) = \frac{3}{4}[1 + x^2 + (x^3 + x^{-1})\arctan x]$ being the Kawasaki function. The constant R is a universal ratio of dynamic amplitudes and its value depends on the theories involved. Siggia, Halperin, and Hohenberg *et al.* [45] predict $R = 1.20$. We will discuss these findings in connection with recent data obtained from polymer-solvent systems [30] in Sec. V.

III. EXPERIMENTAL SECTION

A. Light scattering experiment

1. Characterization of the polymers used

The synthesis of the polymers used in this study is described elsewhere [47]. The molecular weights were determined by light scattering from solutions in toluene and the molecular weight distributions were measured by gel permeation chromatography using calibration by siloxane standards. The respective parameters are summarized in Table II. Relevant parameters not differing with N (index of refraction n, density ρ) are given in Ref. [18].

2. Sample preparation

According to the theoretical (mean field) prediction the critical volume fraction ϕ_c of PEMS is given by $\phi_{c,\mathrm{PEMS}} = N_{\mathrm{PDMS}}^{1/2} / (N_{\mathrm{PDMS}}^{1/2} + N_{\mathrm{PEMS}}^{1/2}) = 0.456$. Proper amounts of polymers were dissolved in n-hexane and filtered through Millipore filters (0.22 μm) into a 20 mm o.d. dust free light scattering cell. To remove the solvent, the sample was held under vacuum for several days at 80 °C. The cloud point was independently checked by a polarization microscope to be a $T = 28.74$ °C. This value is in agreement with the T_c found for the previously studied system [18] on the basis of the T dependence of $\chi_0 = 2/N$ [47].

3. Apparatus

Light scattering experiments were performed in the temperature range $8 \times 10^{-4} < \varepsilon < 4 \times 10^{-2}$ and in the momentum transfer range q ($q = 4\pi n / \lambda \sin\theta/2$, with θ being the scattering angle) of $9.4 \times 10^{-4} < q/\text{Å}^{-1} < 3.6 \times 10^{-3}$ using a laser light scattering goniometer from ALV (Langen, Germany). The temperature control was achieved by a thermostat (Julabo F-30-MH) with a precision of ± 0.01 K. The light source was an argon ion laser (Spectra Physics model 165) operating at $\lambda = 488$ nm. The intensity of the primary beam ($\cong 10$ mW) was monitored with a photodiode in order to correct for fluctuations in the laser power. The transmitted light was also measured by another photodiode to calculate the transmission (see below). Scattered light was detected using a photomultiplier (PM) (EMI 9863). Because of the slow dynamics the intensity at each angle was integrated over 6 min. Prior to measurements the sample was annealed for 2 h to achieve thermal equilibrium. The mea-

TABLE II. Degree of polymerization N, molecular weight M_W, and polydispersity $u = M_W/M_n - 1$ of the polymers used in this study.

Polymer	N	M_W	u
PDMS	225	16800	0.06
PEMS	325	28800	0.06

sured intensity was corrected for dark counts of the PM tube, dead time of the electronic system, and the usual angular dependence of the scattering volume. The alignment of the system in the whole θ range with respect to the intensity of toluene ($R_{VV}^{\text{toluene}}=3.96\times10^{-6}$ cm^{-1} at $\lambda=488$ nm [48]) was reproducible within $\pm1.5\%$. The incident and the scattered laser beam were polarized perpendicular to the scattering plane, so that the geometry of the measurement was the so-called VV geometry. The full autocorrelation function of order parameter fluctuations were measured with an ALV-3000 correlator.

B. Data treatment

1. Turbidity correction

The usual relationship between structure factor and light scattering intensity (see Sec. III B 2) is only valid if the effects of turbidity and multiple scattering can be ignored. However, close to the critical point this may not be the case, because then a significant amount of light is scattered hence reducing the intensity of the light I_{trans} passing through. This can be simply formulated by Lambert-Beer's law

$$I_{\text{trans}}=I_0\exp(-\tau d)\ , \tag{3.1}$$

where τ is the turbidity and d is the path length of the light through the sample. I_{trans} and I_0 are determined experimentally (see Sec. III A), hence τ can be deduced. On the basis of an OZ ansatz, Puglielli and Ford [49] obtained for the turbidity

$$\tau=A'S(\mathbf{q})H(k_i\xi)\ , \tag{3.2}$$

where A' is a constant and the function $H(y)$, where $\mathbf{k}_i=2\pi n/\lambda$, is given by

$$H(y)=\left[\frac{8y^4+4y^2+1}{8y^6}\right]\ln(1+4y^2)-\left[\frac{2y^2+1}{2y^4}\right]\ . \tag{3.3}$$

Our experimental data of the turbidity τ obtained by Eq. (3.1) is adequately fitted by

$$\tau=A\,\varepsilon^{-1.24}H(1.82\times10^5\varepsilon^{-0.62})\ , \tag{3.4}$$

where A is a constant that is treated as a fit parameter. Figure 2 shows a plot of τ as a function of the reduced temperature ε using Eqs. (3.2) and (3.3). The critical exponents are those from Table I.

The correction due to double scattering can be estimated via [27]

$$I=I_0\left[\frac{\partial\varepsilon}{\partial\phi}\right]^2 S(\mathbf{q})[1-(1-R)\tau l]\ , \tag{3.5}$$

where R is the double scattering correction and l is the path length of the scattered beam [$2l=d$ in Eq. (3.1)]. In the basis of our experimental result for τ we can estimate by interpolation from data by Shanks and Sengers [50] for $\varepsilon=10^{-3}$ a value of $R\cong0.04$. Inserting this value into Eq. (3.5) shows that no multiple scattering correction is needed. What is left is the comparison with our previously published data [18]. There we had found $\tau=2.5\%$ for $q\xi=1$, which is for $\lambda=633$ nm and $\theta=90°$ at $\sim\ln\varepsilon=-2$. In this study we find for the same value of ε, $\tau=8.5\%$ taking into account the differences in the path lengths by a factor of 2. Correcting for the different wavelengths (here 488 nm) we find $\tau\cong3\%$. The remaining uncertainty may be related to the error in determining T_c in the previous study. Hence both samples are comparable.

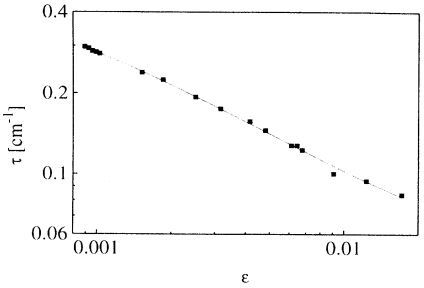

FIG. 2. The measured turbidity τ according to Eq. (3.1) as a function of reduced temperature ε(■). The full line is a fit of Eq. (3.4) to the data with free parameter A.

2. The static structure factor

The static structure factor $S(\mathbf{q})$ is obtained from the angular dependent $I(\mathbf{q})$ by

$$S(\mathbf{q})=\frac{I(\mathbf{q})\lambda^4\bar{\rho}N_L R_{VV}^{\text{ref}}}{I_{\text{ref}}n_{\text{ref}}^2 4\pi^2(n_A-n_B)^2\bar{M}_{\text{mon}}}\ , \tag{3.6}$$

where ref means reference sample (= toluene, see Sec. III A), λ is the probing wavelength, $\bar{\rho}=\phi_A\rho_A+\phi_B\rho_B$, and n is the index of refraction. $\bar{M}_{\text{mon}}=\phi_A M_{\text{mon}}^A$

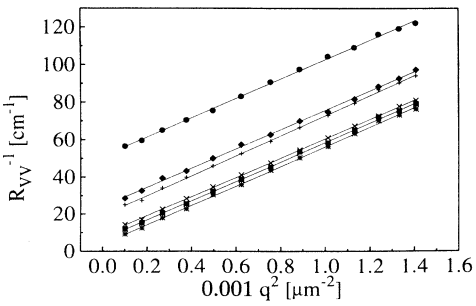

FIG. 3. The reciprocal Rayleigh ratio versus the square of the momentum transfer for various temperatures according to Eq. (2.7). From the bottom to the top $T=302.17$ K (★), $T=302.31$ K (■), $T=302.46$ K (x), $T=302.86$ K (+), $T=303.16$ K (♦), $T=304.16$ K (●). The critical temperature is $T=301.90$ K.

$+\phi_B M^B_{\rm mon}$. Since we report data only in the vicinity of T_c, no corrections for a background due to density fluctuations were undertaken which are typically four orders of magnitude smaller. In Ref. [18] we had reported data yielding Rayleigh ratios down to $\cong 100$ cm^{-1}. In Fig. 3 we show $R_{vv}^{-1}(\mathbf{q}) \propto S(\mathbf{q})^{-1}$ vs q^2 based on an OZ approximation [cf. Eq. (2.7)] for our data which go below 10 cm^{-1} close to T_c, which is one order of magnitude higher scattering intensity than we had previously due to a smaller ε we have reached here. In our case $\varepsilon_{\rm min} \cong 8\times 10^{-4}$, in the previous paper [18] $\varepsilon_{\rm min} \cong 5\times 10^{-3}$ which gives an order of magnitude in $S(\mathbf{q})$. As one can see from Fig. 3, the OZ theory gives a good representation of the data as expected [26].

3. *The Rayleigh linewidth [51]*

The desired correlation function of the scattered electric field $g(\mathbf{q},t)$ is related to the measured intensity time correlation function $G(\mathbf{q},t)$ through the Siegert relation

$$G(\mathbf{q},t)=\langle I(\mathbf{q})\rangle^2[1+f\alpha^2|g(\mathbf{q},t)|^2] , \tag{3.7}$$

where $\langle I(\mathbf{q})\rangle$ is the mean intensity, f is an instrumental factor, and α is the fraction of the totally scattered intensity $I(\mathbf{q})$ arising from concentration fluctuations. $g(\mathbf{q},t)$ is identified as the concentration autocorrelation function, which is further given by

$$g(\mathbf{q},t)=\frac{S(\mathbf{q},t)}{S(\mathbf{q})} , \tag{3.8}$$

where $S(\mathbf{q},t)$ is the dynamic structure factor and $S(\mathbf{q})$ is given by Eq. (3.6) and Eq. (2.5) subsequently. The time evolution of $S(\mathbf{q},t)$ is given by

$$S(\mathbf{q},t)=S(\mathbf{q},t=0)\exp(-\Gamma t) \tag{3.9}$$

with Γ being the Rayleigh linewidth. It is related to the mutual diffusion coefficient D_c by

$$\Gamma=D_c q^2 . \tag{3.10}$$

As has been discussed elsewhere [18], the Rayleigh linewidth Γ has to be composed into a critical part Γ_c and a background part Γ_B,

$$\Gamma=\Gamma_c+\Gamma_B . \tag{3.11}$$

However, the background contributions (not to be confused with the background due to density fluctuations) are, as has been shown [18], for polymer blends for values of $\varepsilon<0.01$ already small (less than 10% on the basis of Fig. 13 in Ref. [18]). Furthermore, the difference becomes progressively large since $\Gamma_c \propto \varepsilon^{\nu}$ and $\Gamma_B \propto \varepsilon^{\gamma}$. We will study dynamical effects entirely in the strong fluctuation limit, starting at $\sim\varepsilon<7\times 10^{-3}$, estimated on the basis of the crossover analysis (see Sec. IV). For the latter ε value the ratio of Γ_c/Γ_B can be estimated to be 20. In the region where the determination of η was performed (see Secs. IV and II A) the difference is typically a factor of 50 (at $\varepsilon\cong 10^{-3}$), corresponding to an error of at most 2%. Consequently, no background correction was undertaken.

IV. STATIC PROPERTIES: RESULTS

It is well known that close to T_c even polymer systems are not mean field systems but behave like three-dimensional Ising systems [9,10,13,14,16–18, 21,25]. The criterion that separates these two cases is the Ginzburg criterion [52–54]. However, unless a proper crossover function was introduced [20], the data had been analyzed in the two extremes, thereby force fitting the temperature dependence of the susceptibility to the mean field exponent $\gamma=1$ by choosing the proper mean field critical temperature [24]. We know [20,24], that applying the crossover function by Belyakov and Kiselev [22] leads to a more appropriate data description and leads to a reliable determination of the Ginzburg number Gi which tells us when fluctuation effects are dominant. This is equivalent with the region where the polymer topology is unimportant since the correlation length of order parameter fluctuations, largely exceeds the coil dimensions. We shall first try, on the basis of the crossover analysis, to clearly find the region $\varepsilon<\mathrm{Gi}$.

The crossover function we use is an explicit solution to first order in the perturbation parameter $\varepsilon=4-d$ (d being dimensionality) based upon a renormalization group analysis. It reads

$$\hat{\varepsilon}=[1+2.333\hat{S}(\mathbf{0})^{\Delta/\gamma}]^{(\gamma-1)/\Delta} \times\{\hat{S}^{-1}(\mathbf{0})+[1+2.333\hat{S}(\mathbf{0})^{\Delta/\gamma}]^{-\gamma/\Delta}\} \tag{4.1}$$

with $\hat{\varepsilon}=\varepsilon/\mathrm{Gi}$ and $\hat{S}(\mathbf{0})=a_0 S(\mathbf{0})\mathrm{Gi}$. a_0 is defined later, Gi is the Ginzburg number. The critical exponents are those for the three-dimensional (3D) Ising case $\gamma=1.24$ and $\Delta=0.51$, where the latter exponent determines the correction to first order to the power laws that describe the singularities at T_c [55]. The constant a_0 is given by the amplitude of the squared term of the order parameter $\psi(\mathbf{r})=\phi(\mathbf{r})-\phi_c$ in the Landau-Ginzburg-Wilson formulation of the free energy ΔF for a second order phase transition

$$\frac{\Delta F}{kT}=\int_v d^3\mathbf{r}\left[\frac{1}{2}a_0\varepsilon'\psi(\mathbf{r})^2+\frac{1}{4!}u_0\psi(\mathbf{r})^4+\frac{1}{2}c_0[\nabla\psi(\mathbf{r})^2]\right] \tag{4.2}$$

with ε' being the reduced temperature (with the mean field T_c). a_0 can be expressed in quantities of the random phase approximation to be [16]

$$a_0=(N_A V_A\phi_A)^{-1}+(N_B V_B\phi_B)^{-1}-2\chi_B\bar{V}^{-1} . \tag{4.3}$$

Here V_i are the monomer volumes and $\bar{V}=(V_A V_B)^{1/2}$. χ_B is reminiscent of the Flory-Huggins lattice model as it is given by the entropic contribution of the Flory-Huggins χ parameter $\chi=\chi_A/T+\chi_B$. For a discussion see, e.g., Ref. [15]. The Ginzburg number Gi is defined in the light of the coefficients appearing in Eq. (4.2) to be [22,23,25]

$$\mathrm{Gi}=\frac{1}{18\pi^2}\left[\frac{3}{4\pi}\right]^2\frac{u_0^2}{a_0^4}\left[\frac{\bar{V}}{\xi_0^3}\right]^2\frac{1}{N_L^2} , \tag{4.4}$$

where ξ_0 is the bare correlation length which must be

consistent with $c_0 = a_0 \xi_{50}^2$. The value of Gi controls the crossover such that for $\varepsilon \ll \mathrm{Gi}$, Ising behavior for the susceptibility is observed and mean field behavior is observed for $\varepsilon \gg \mathrm{Gi}$. This has already been shown for a great variety of binary blends with vastly differing degrees of polymerization [20,24]. From a fit of Eq. (4.1) to our corrected susceptibility data (for corrections, see Sec. III B) shown in Fig. 4 the parameters Gi and a_0 are obtained. The value for Gi amounts to $\mathrm{Gi} = 6.88 \times 10^{-3}$. This value is in good agreement with values of Gi as obtained from various other systems [24]. In Fig. 4 the fat symbols belong to $\varepsilon < \mathrm{Gi}$, the shallow ones to $\varepsilon > \mathrm{Gi}$ since the crossover naturally occurs at $\mathrm{Gi} = \varepsilon$. Only data for $T < T(\mathrm{Gi})$ will be used for the following scaling analysis. The numerical value for Gi corresponds to a T width of $T(\mathrm{Gi}) - T_c = 2.1$ K. At $T(\mathrm{Gi})$, the correlation length ξ is in the order of 300 Å, which is roughly one order of magnitude larger than the coil dimensions, so definitely the polymeric nature of the system is lost with respect to the magnitude of the order parameter fluctuations. Having established now the 3D Ising regime, the strong fluctuation limit, we perform fits of $S(\mathbf{0})$ and ξ, as obtained via Eq. (2.7), following Eqs. (2.6) and (2.4), respectively. The result for $S(\mathbf{0}) = S_0 \varepsilon^{-\gamma}$ is shown in Fig. 5, the result for $\xi = \xi_0 \varepsilon^{-\nu}$ is shown in Fig. 6. The resulting parameters for γ and ν are listed in Table I. The obtained value for $\xi_0 = 14.9$ Å is in agreement with data published recently [24] on the basis of the N scaling of ξ_0. Furthermore, we get for S_0 a value of $S_0 = 35.7$. After conversion into the units as given in Ref. [24] (there S_0 is named C^+) we obtain $C^+ = 2940$ cm^3/mol which is in reasonable agreement with the reported values there on the basis of the N scaling of C^+. The value of the critical temperature T_c was also found to be consistently $T_c = (301.90 \pm 0.01)$ K both from Fig. 5 and Fig. 6 in a first run allowing for three free parameters in fitting Eqs. (2.4) and (2.6), respectively. Then subsequently, the T_c was fixed and the fits shown in Figs. 5 and 6 were obtained, the exponents shown in Table I.

Since we are in a regime for which $\varepsilon \ll \mathrm{Gi}$, and hence the 3D Ising universality class is obeyed, we may further

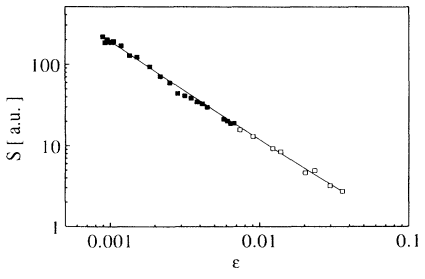

FIG. 4. The static susceptibility $S(\mathbf{0})$ as a function of the reduced temperature ε. The full curve is a fit of Eq. (4.1) to the data. Full points (■) are for $\varepsilon < \mathrm{Gi}$, shallow points (□) for $\varepsilon > \mathrm{Gi}$. Fit parameters are a_0 and Gi. The critical temperature is obtained (consistently) from scaling fits of ξ and $S(\mathbf{0})$ according to Eqs. (2.4) and (2.6), respectively, only in the vicinity of T_c.

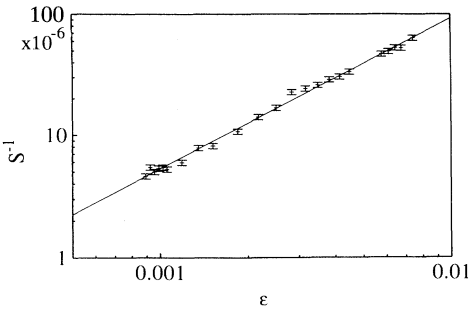

FIG. 5. Double logarithmic plot of $S(\mathbf{0}) = 35.7 \times \varepsilon^{-1.24 \pm 0.02}$ according to Eq. (2.6) in the range $\varepsilon < \mathrm{Gi}$ according to the crossover fit presented in Fig. 4.

determine the critical exponent η [see Eq. (2.2)], which describes the decay of correlation at T_c. As already stated (Sec. II), if $q\xi$ is not too large [26], the OZ ansatz is still useful, we may write formally

$$\xi^2 S(\mathbf{0})^{-1} = S_0^{-1} \xi_0^2 \varepsilon^{-\nu\eta} = \mathrm{const} \times \xi^{\eta} \tag{4.5}$$

thereby using the hyperscaling relation $(2-\eta)\nu = \gamma$ [56]. Thus, a plot of $\xi^2 S(\mathbf{0})^{-1}$ versus ξ should yield the critical exponent η, which is shown in Fig. 7. We obtain a value $\eta = 0.036 \pm 0.002$ which is in agreement with the theoretical value listed in Table I. A similar procedure was performed by Janßen, Schwahn, and Springer [14], however, they obtained $\eta = 0.047 \pm 0.004$, which exceeds the theoretical value. This seems to be a typical finding for results obtained from neutron scattering, as was argued by Chang, Burstyn, and Sengers [27]. Not only must $q\xi$ be large to get the true asymptotic form of the structure factor but also should q be small enough so that the short range order is not seen. In Eq. (2.2) the conditions are $T = T_c$ and r large, a fact that is better fulfilled by light scattering (almost one decade smaller q) than with neutrons. The experimental facts so far have been summarized by Schwahn, Belkoura, and Woermann [57]. Our above presented analysis (Fig. 7) uses the fact that for light scattering q is much smaller and although the $q\xi$ range here and in Ref. [14] is almost equal we obtain a more satisfying result.

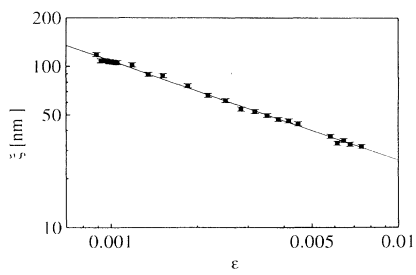

FIG. 6. Double logarithmic plot of $\xi = 14.9 \times \varepsilon^{-0.62 \pm 0.01}$ with ξ in Å according to Eq. (2.4) in the range $\varepsilon < \mathrm{Gi}$ (see also Fig. 5).

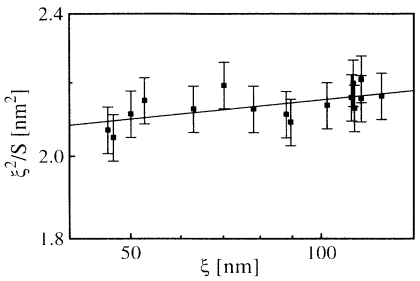

FIG. 7. Double logarithmic plot of $\xi^2 S^{-1}(0)$ versus ξ for $\varepsilon < \mathrm{Gi}$. The straight line has the slope $\eta = 0.036 \pm 0.002$ according to Eq. (4.5).

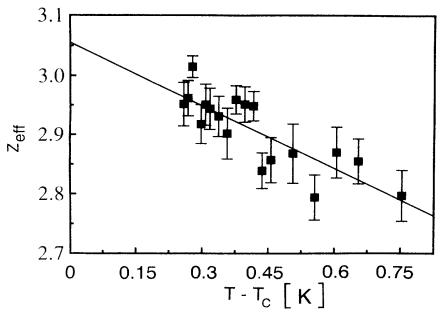

FIG. 8. Plot of z_{eff}, as obtained from the angular dependence of the Rayleigh linewidth according to Eq. (5.1) versus the temperature difference $T - T_c$. From a linear extrapolation toward T_c, the exponent $z = 3.06 \pm 0.03$ is obtained.

One final comment needs to be added concerning the question whether the condition $T = T_c$ in Eq. (2.2) needs further clarification. One might argue that although we analyze our data only for $\varepsilon < \mathrm{Gi}$ the critical exponent for susceptibility is not entirely given by the value for γ as listed in Table I, because there is a crossover which is specific for polymer systems and what is seen instead is an effective susceptibility exponent $\gamma_{\mathrm{eff}} = \partial \log \hat{S}^{-1}(\mathbf{0}) / \partial \log \hat{\varepsilon}$ as derived from Eq. (4.1). However, for $\varepsilon = \mathrm{Gi}$ we find $\gamma_{\mathrm{eff}} \cong 1.232$ (Fig. 7 of Ref. [23]), hence the difference between γ_{eff} and γ from Table I is in the order of the error in determining η. Furthermore, crossover in $S(\mathbf{0})$ and ξ look the same [18,25], so that the hyperscaling relation may be used throughout for $\varepsilon < \mathrm{Gi}$. Deutsch and Binder [25] have argued that the crossover in the order parameter with critical exponent $\beta [\psi(\mathbf{r}) = \psi_0 |\varepsilon|^{\beta}]$ may differ from those in $S(\mathbf{0})$ and ξ. However, that is experimentally a difficult but challenging task. In summary, the analysis presented above is, to our knowledge, the first determination of η from a polymer blend in agreement with theoretical predictions for the 3D Ising universality class.

V. DYNAMIC PROPERTIES: RESULTS

As already outlined in Sec. II B, we will concentrate only on the region where mode coupling effects occur. Reading from Fig. 1 that is given by $\xi / R_g > N^{1/2}$, hence for $\varepsilon < \mathrm{Gi}$. In this region it is found [cf. Eq. (2.11)] that $\Gamma(\mathbf{q}) \propto (q\xi)^3$. However, a crossover is associated with any line drawn in Fig. 1, so that basically we may write

$$\Gamma(\mathbf{q}, T) \propto q^{z_{\mathrm{eff}}(T)} , \tag{5.1}$$

where the value of z_{eff} for $T = T_c$ is given by Eq. (2.13). In Fig. 8, we show z_{eff} plotted versus $T - T_c$ and get a value of z by linear extrapolation for $T \to T_c$ being $z = 3.06 \pm 0.03$. According to Eq. (2.13), this is in agreement with the theoretical value [45] for $x_\eta = 0.065$ and in accord with other experimental findings [44].

Solving the linearized hydrodynamic equations of a binary liquid lead to five hydrodynamic modes [58]: four diffusive ones and a propagating one (Brillouin). The diffusive modes consist of a thermal diffusion mode, a concentration diffusion mode, and a viscous relaxation mode for the two transverse components of the momentum density. All three modes are characterized by respective diffusion constants. D_T for the thermal diffusion (heat transport), D_c for the concentration diffusions, also called mutual or interdiffusion, cf. Eq. (3.10) (mass transport), and D_v, the viscous diffusion constant (momentum transport). They are connected to specific transport coefficients via

$$D_T = \frac{\lambda_T}{C_P} , \tag{5.2a}$$

$$D_c = \frac{\Lambda_0}{S(\mathbf{q})} , \tag{5.2b}$$

$$D_v = \frac{\eta_s}{\chi_p} . \tag{5.2c}$$

λ_T is the thermal conductivity, C_p is the constant pressure specific heat, Λ_0 is identified by Eq. (2.9) together with Eq. (3.10), $S(\mathbf{q})$ is given by Eq. (2.7), η_s is the shear viscosity and χ_p is the susceptibility for the momentum density. The transport coefficient of heat exhibits the following scaling law (for $\mathbf{q} \to \mathbf{0}$):

$$\lambda_T = \lambda_0 \xi^{x_\lambda} , \tag{5.3}$$

whereas the scaling law for η_s is given by Eq. (2.12). Among the coefficients x_λ, x_η, and η the relation [32]

$$x_\lambda + x_\eta = 4 - d + \eta \tag{5.4}$$

holds. Hence we may predict the value of x_λ from our data for x_η (Fig. 8) and η (Fig. 7) to be $x_\lambda = 0.976$. Concerning the reliability of this result we may argue in the same way here as we had discussed in the determination of η (Sec. IV).

For the mass transport coefficient, the Onsager coefficient, the following scenario holds: Combining Eqs.

(3.10) and (2.9) we write for $\mathbf{q}=\mathbf{0}$,

$$\Lambda=\frac{\Gamma}{q^2}S(\mathbf{0}) . \tag{5.5}$$

Now, clearly if Γ/q^2 does not depend on ξ, mode coupling effects otherwise occur in the sense of nonlocal diffusion as introduced by Perl an Ferrell [59], then one easily shows, using the RPA formalism

$$\Lambda=\text{const}\times\frac{\Gamma}{q^2}\left[\frac{T-T_c}{T}\right]^{-1}\propto(q^2\varepsilon)^{-1} \tag{5.6}$$

which is the large region in the right lower part of Fig. 1. However, if mode coupling comes into play, then the quantity Γ/q^2 depends on ξ according to the arguments thoroughly presented in Ref. [18]. Basically in the so-called hydrodynamic regime (in Fig. 1 the region $q^2\varepsilon^{\nu})\Gamma/q^2\propto\xi^{-1}$ and hence $\Lambda\propto\xi$ on the basis of Eq. (5.5) because $S(\mathbf{0})\propto\xi^2$ in that region. This has been observed quantitatively and is well established [18]. What remained to be established is the crossover form $q^2\varepsilon^{\nu}$ to $q^3\varepsilon^{\nu x_\eta}$. For that data close to T_c is needed. Formally, if we expand Eq. (2.11) for $q\xi\gg1$, then we obtain $\Gamma/q^3=\text{const.}\propto kT/6\pi\eta_s$. Inserting herein for η_s Eq. (2.12) we get for $\Lambda[\propto\Gamma$, cf. Eqs. (5.2b) and (5.5)]

$$\Lambda\propto\eta_0\xi^{-x_\eta}\propto\varepsilon^{\nu x_\eta} \tag{5.7}$$

which is the regime $q^3\varepsilon^{\nu x_\eta}$ in Fig. 1 in the upper right part. This crossover from $\Lambda\propto\varepsilon^{\nu}$ to $\Lambda\propto\varepsilon^{\nu x_\eta}$ is shown in Fig. 9. We have plotted Λ versus ε double logarithmically together with the two limiting slopes $\nu=0.62$ and $\nu x_\eta=0.041$. According to Fig. 1 the crossover occurs at $q\xi=1$. On the basis of our q range used we have taken an average value being at a ξ of about 600 Å to fulfill $q\xi=1$. This value $\bar{q}\xi=$ is indicated by an arrow in Fig. 9. Although we have focused our attention only to the T range close to T_c it is difficult to unambiguously extract the value of νx_η from the data. Figure 10 displays the data for Λ for the smallest $\varepsilon(<1.5\times10^{-3})$. The straight line is a fit to the data yielding $\nu x_\eta=0.058\pm0.011$. This

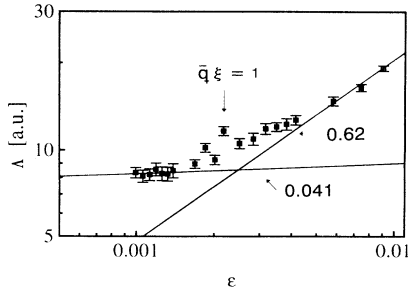

FIG. 9. The Onsager coefficient Λ versus the reduced temperature. Shown is the crossover from $q^2\varepsilon^{\nu}$ to $q^3\varepsilon^{\nu x_\eta}$ ($\nu=0.62$, $\nu x_\eta=0.041$) which occurs at $\bar{q}\xi=1$ for $\xi>R_g\sqrt{N}$ and $(qR_g)^{-1}>\sqrt{N}$. This crossover means that we are already so close to T_c that Γ/q^3 is constant, so only the (weak) divergence of the viscosity is seen.

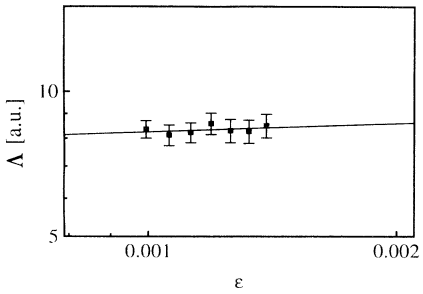

FIG. 10. The Onsager coefficient Λ versus the reduced temperature for $q\xi\gg1$. Here we find $\Lambda\propto q^3\varepsilon^{\nu x_\eta}\propto\varepsilon^{0.058\pm0.01}$ which is the slope of the straight line.

is higher than the theoretical expectation for $\nu x_\eta=0.63\times0.065=0.041$.

Further, on the basis of Fig. 1 the crossover between mean field and Ising is located where mode coupling effects occur. We read from Fig. 1 that this should happen for $\xi=R_g\sqrt{N}=650$ Å. This length corresponds to $\varepsilon\cong3\times10^{-3}$. On the other hand, from our crossover analysis (see Sec. IV) we obtain a Ginzburg temperature of $T(\text{Gi})=304$ K being $\varepsilon=7\times10^{-3}$. The obtained agreement is rather good bearing in mind that one degree less $T(\text{Gi})$ is sufficient to almost match the two resulting ε values completely. So we conclude that within the errors involved in our data, agreement with Binder [33] is obtained on the basis of the evaluation of Gi with the crossover function formalism.

Furthermore, using the exponent x_η, obtained by Fig. 7, we have fitted Eq. (2.15) to the data. For the determination of Γ^* [cf. Eq. (2.14)] the mixing rule for η_s has been employed, which we had already used in Ref. [18]. The result is shown in Fig. 11. The agreement is similarly better than what we have published previously [18]. However, if we use $R=1.20$ as is proposed by Siggia, Halperin, and Hohenberg [45], the data shows a systematic discrepancy with respect to the theoretical curve. This is in variance with the result by Miyashita and Nose

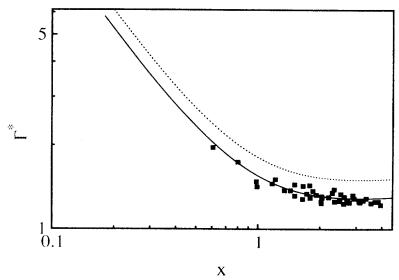

FIG. 11. The scaled linewidth Γ^* according to Eq. (2.15) versus $x=q\xi$. The dashed line is obtained using $R=1.2$ instead of $R=1.03$ (full line). Clearly, the data is not compatible with $R=1.2$.

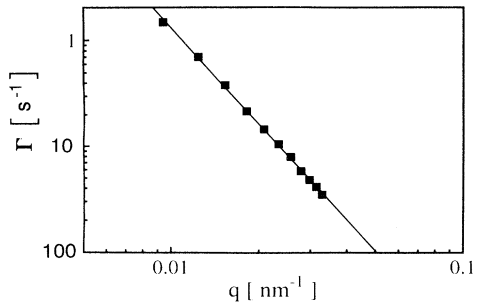

FIG. 12. The Rayleigh linewidth according to Eq. (3.9) versus q. The straight line has a slope of 3 ± 0.03.

[30] who found that for the polymer-solvent system the data is compatible with $R=1.20$.

According to Fig. 1 we may observe for $\xi > R_g\sqrt{N} > 650$ Å the crossover from $q^4\varepsilon^{\nu x_\eta}$ to $q^3\varepsilon^{\nu x_\eta}$ or to put it easier from a q^4 to a q^3 scaling of Γ for $(qR_g)^{-1} > \sqrt{N}$. In order to check this we choose a temperature very close to T_c, namely $T-T_c=0.24$ K, where $\xi > 2000$ Å. The obtained variation in q allows for a variation in $(qR_g)^{-1}$ to be $(qR_g)_{\max}=0.15 > N^{-1/2}=0.06 > (qR_g)_{\min}=0.03$. According to this, we should be able to see a crossover from q^3 to q^4 for large q. The result is shown in Fig. 12, where the rate is plotted versus q. The straight line has a slope of $z=3.00\pm0.03$, which means that we do not see any crossover. We offer the following explanation for this finding: One might argue that the prefactors determining the exact numerical values are usually omitted in Fig. 1, so that basically we are not in the proper range of $(qR_g)^{-1}$. However, on the other hand, a scaling $\Gamma \propto q^4\varepsilon^0$ without mode coupling is exactly what is predicted by Eq. (2.10), which is basically the behavior of the nonmode coupled background which shows a critical slowing down according to van Hove theory. This is hidden in our data in the background which has been extensively argued about in Ref. [18], and which has not been corrected for here (see Sec. III B). The line of argumentation should be reversed: The experimental finding that Fig. 12 shows a clear $\Gamma \propto q^3$ behavior in the whole q range investigated, is a strong indication for the neglecting of any background contributions so close to T_c. Hence, according to Eq. (3.11), $\Gamma_c \cong \Gamma$ is a very good approximation. For $\varepsilon \ll \mathrm{Gi}$ mode coupling occurs throughout, and consequently the background contributions are only possible to detect for extremely large q, possibly not accessible by light scattering.

VI. DISCUSSION

As already addressed in the introduction we are mainly concerned with two questions: First, to what extent are binary blends and polymer-solvent systems comparable with respect to their critical behavior and second, to which universality class in the sense of Hohenberg and Halperin (HH) [32] do binary polymer blends belong? Let us first discuss the latter question.

Concerning this item, Tanaka [31] has raised considerable questions, especially with respect to the coupling of order parameter fluctuations and viscoelastic forces. Classical fluids including binary liquid mixtures and simple fluids belong to the model H of HH. The kinetic equations for binary liquid mixture are given by [58]

$$\frac{\partial\phi}{\partial t} = -\nabla(\phi v) + L_0\nabla^2\frac{\delta F}{\delta\phi} + \Psi \tag{6.1}$$

and the Navier-Stokes equation

$$\rho\frac{\partial v}{\partial t} = -\nabla\Pi - \nabla p_1 + \eta_s\nabla^2 v + \zeta \ . \tag{6.2}$$

Here ϕ and v are the concentration and velocity fields, respectively, and Π is the stress tensor caused only by the fluctuations of ϕ. ρ is the density, p_1 is a part of the pressure and η_s is the viscosity. Ψ and ζ are random forces. F is given by Eq. (4.2). Newtonian fluids are adequately described by these basic hydrodynamic equations (mass and momentum conservation). However, they are only valid on time scales larger than any characteristic viscoelastic time of the system [31]. That may be complex internal degrees of freedom (i.e., disentanglement time) or the glass transition phenomena. That leads to substantial changes in Eqs. (6.1) and (6.2), such that, according to Doi and Onuki [60], a stress tensor $(\nabla\sigma^{(n)})$ has to be added, which means that the motion of a polymer relative to the solvent is driven not only by the gradient of the osmotic pressure [cf. Eq. (6.2)] but also by the gradient of the network stress $\sigma^{(n)}$. We make the assumption that this may also hold if dynamically one polymer has a vastly different glass transition than the other, so that the faster one may be treated as a solvent. The network stress arises from the point that the stress in polymer systems is supported by the structure and thus a gradient in $\sigma^{(n)}$ causes a net force on the chains leading to a motion of chains relative to the solvent.

That is what is meant with coupling between order parameter fluctuations and viscoelastic forces. Via a constitutive equation [61]

$$\sigma_{ij}^{(n)} = \int_{-\infty}^{t} dt' G(t-t')\kappa_{ij}^{(p)}dt' \ , \tag{6.3}$$

where κ_{ij} is the shear rate and $G(t)$ is the shear relaxation modules, we can further relate $G(t)$ to the viscosity

$$\eta_s \propto \int_0^\infty G(t)dt \ . \tag{6.4}$$

We see directly that the viscosity behavior is likely a sensitive sensor for any deviations from the model H of HH. For our particular system here, this seems not to be important. According to Tanaka [31], we may estimate the ratio between τ_ξ/τ_t, the ratio between the decay time of fluctuations τ_ξ and the characteristic rheological time τ_t to be $\tau_\xi/\tau_t \cong N^{1/2}\varepsilon^{-3/2}$ being always larger than one. That means, in our systems the order parameter fluctuation are always the slowest relaxing variable close to T_c. Dynamic asymmetry in polymer blends are not as important as glass transition phenomena, so our system behaves "ideally" in the sense of model H of HH. Consequently, all scaling parameters are in accord with theory,

especially the most crucial one, the viscosity divergence, although an exact theory, which relates the occurrence of viscoelastic coupling to the extent to which viscosity scaling exponents are reformulated, is not known to us. In the following we may add some speculations, which are not supported theoretically, but we find them interesting to report.

The above arguments may be further supported by a recent study on the interdiffusion dynamics in a PDMS-PEMS blend [62], where it has been found that the concentration dependence of the interdiffusion coefficient follows the so-called fast mode approach which allows for different diffuse segment fluxes in a sense of a Hartley-Crank type of equation [63]. It is contrasted to the slow mode ansatz which may be derived under the condition of microscopic compressibility as it may describe the interdiffusion of two solids with infinite viscosity. A theoretical approach by Akcasu, Naegele, and Klein [64] allows one to interpolate between both cases by varying the compressibility of the system, i.e., the distance from the glass transition, where then coupling effects in the sense of Tanaka may occur if the T_c of the system is chosen properly. Interestingly, now that the interdiffusion in PS-PPMS [poly(styrene)-poly(phenylmethylsitoxane)] was found to follow the slow mode [51], where indeed glass transition effects occur. In this latter system the (PS) component exhibits a glass transition close to the region of measurement.

We may further note that the reported anomaly [24] of the Ginzburg number as a function of N, namely an unpredicted overshoot of the T (Gi)-T_c difference as compared with other systems (cf. Ref. [24]) is entirely due to PS-PPMS systems. For the other systems studied, it can be easily shown that glass transition effects are negligible. From all that we speculate: It is usually a polymeric component involved (PS) exhibiting a relatively high glass point so that kinetic coupling with the order parameter fluctuations may occur. However, that has to be quantitatively proven in any particular case and is a task for future work. We have to come back to our very first question concerning the comparison between blends and polymer-solvent systems. The possible equivalency between binary blends and polymer-solvent systems is doubted intuitively, because a main assumption in blends is the validity of the so-called Gaussian approximation [65]. This is entirely different in dilute solutions and concentrated solutions because there the excluded volume effects have to be properly taken into account. The Gaussian assumption, on the other hand, is only valid for a small excluded volume or high concentrations, possibly melts.

The viscosity behavior of polymer-solvent systems has been exemplarily studied in Ref. [30]. There $R=1.2$ in Eq. (2.15) was found to adequately describe the linewidth data. Miyashita and Nose [30] state that the theoretical value of $R=1.20$ is intuitively more acceptable, since the diffusion coefficient would satisfy a Stokes-Einstein diffusion law with prefactor $1.2/6\pi \cong 1/5\pi$ in accordance with Stokes's law for a spherical droplet with radius ξ moving in a medium with the same viscosity as that of a liquid droplet. However, that numerical prefactor $1/5\pi$ was not confined by the vast majority of experiments [66]. We speculate that in Ref. [30] the value of η_s entering the expression for the scaled linewidth, in analogy to Eq. (2.15), was calculated using improper assumptions, i.e., a wrong mixing rule for the solution viscosity. Further, we note that in polymer-solvent systems the proper determination of the background causes considerable problems [67] which makes it difficult to distinguish unambiguously between the two R values [30,68].

Finally, the usual agreement between blends and polymer-solvent systems with respect to the universality class is doubted mainly on the basis of viscosity data (cf. Ref. [28]). Usually, the critical exponents for solutions are renormalized [69], however, we are not aware of any study that has a close look for the viscosity exponent. Clearly the form of the free energy ΔF via Eq. (4.2) is not valid for solutions. Thus it is not clear what free energy functional will enter Eq. (6.1) and its modifications to transient network stresses, i.e., for concentrations beyond the overlap concentration. It is further not known to what extent then the scaling theoretical of the viscosity may be described. There is need for theoretical work in as much experiments [28] show clear deviation from model H of HH.

We conclude the following:

(1) In the absence of viscoelastic couplings [31], binary polymer blends belong to the universality class H of Hohenberg and Halperin.

(2) This is contrasted to polymer-solvent systems on the basis of the viscosity scaling behavior.

ACKNOWLEDGMENTS

We thank T. A. Vilgis for various helpful comments and illuminations.

[1] G. Ronca and T. P. Russell, Phys. Rev. B **35**, 8566 (1987).
[2] H. Meier and G. Strobl, Macromolecules **20**, 649 (1987).
[3] B. Chu, Q. Ying, K. Linliu, P. Xie, T. Gao, Y. Li, T. Nose, and M. Okada, Macromolecules **25**, 7382 (1992).
[4] Ch. Herkt-Maetzky and J. Schelten, Phys. Rev. Lett. **51**, 96 (1983).
[5] G. Shibayama, H. Young, R. S. Stein, and C. C. Han, Macromolecules **16**, 2179 (1983).
[6] J. S. Higgins and A. I. Carter, Macromolecules **17**, 2197 (1984).
[7] A. Lapp, C. Picot, and H. Benoit, Macromolecules **18**, 2437 (1985).
[8] M. G. Brereton, E. W. Fischer, and Ch. Herkt-Maetzky, J. Chem. Phys. **87**, 6144 (1987).
[9] D. Schwahn, K. Mortensen, and H. Yee-Madeira, Phys. Rev. Lett. **58**, 1544 (1987).
[10] D. Schwahn, K. Mortensen, T. Springer, H. Yee-Madeira, and R. Thomas, J. Chem. Phys. **87**, 6078 (1987).

[11] W. G. Jung and E. W. Fischer, Makromol. Chem. Makromol. Symp. **16**, 281 (1988).
[12] D. Schwahn, K. Hahn, J. Streib, and T. Springer, J. Chem. Phys. **93**, 8383 (1990).
[13] F. S. Bates, J. H. Rosedale, P. Stepanek, T. P. Lodge, P. Wiltzius, G. H. Fredrickson, and R. P. Hjelm, Phys. Rev. Lett. **65**, 1893 (1990).
[14] S. Janβen, D. Schwahn, and T. Springer, Phys. Rev. Lett. **68**, 3180 (1992).
[15] D. Schwahn, S. Janβen, and T. Springer, J. Chem. Phys. **97**, 8775 (1992).
[16] D. W. Hair, E. K. Hobbie, A. I. Nakatani, and C. C. Han, J. Chem. Phys. **96**, 9133 (1992).
[17] P. Stepanek, T. P. Lodge, C. Kedrowski, and F. S. Bates, J. Chem. Phys. **94**, 8289 (1991).
[18] G. Meier, B. Momper, and E. W. Fischer, J. Chem. Phys. **97**, 5884 (1992).
[19] P. G. de Gennes, *Scaling Concepts in Polymer Physics* (Cornell University, Ithaca, 1979).
[20] G. Meier, D. Schwahn, K. Mortensen, and S. Janβen, Europhys. Lett. **22**, 577 (1993).
[21] E. K. Hobbie, L. Reed, C. C. Huang, and C. C. Han, Phys. Rev. E **48**, 1579 (1993).
[22] M. Y. Belyakov and S. B. Kiselev, Physica A **190**, 75 (1992).
[23] M. A. Anisimov, S. B. Kiselev, J. V. Sengers, and S. Tang, Physica A **188**, 487 (1992).
[24] D. Schwahn, G. Meier, K. Mortensen, and S. Janβen, J. Phys. (France) II **4**, 837 (1994).
[25] H. P. Deutsch and K. Binder, J. Phys. (France) II **3**, 1049 (1993).
[26] C. A. Tracy and B. M. McCoy, Phys. Rev. B **12**, 368 (1975).
[27] R. F. Chang, H. Burstyn, and J. V. Sengers, Phys. Rev. A **19**, 866 (1979).
[28] R. F. Berg and K. Gruner, J. Chem. Phys. **101**, 1513 (1994).
[29] J. C. Nieuwoudt and J. V. Sengers, J. Chem. Phys. **90**, 457 (1989).
[30] N. Miyashita and T. Nose, J. Chem. Phys. **100**, 6028 (1994).
[31] H. Tanaka, J. Chem. Phys. **100**, 5323 (1994).
[32] P. C. Hohenberg and B. I. Halperin, Rev. Mod. Phys. **49**, 435 (1977).
[33] K. Binder, Adv. Polym. Sci. **112**, 181 (1994).
[34] G. H. Fredrickson, J. Chem. Phys. **85**, 3556 (1986).
[35] J. J. Binney, N. J. Dowrick, A. J. Fisher, and M. E. J. Newman, *The Theory of Critical Phenomena* (Clarendon Press, Oxford, 1993).
[36] Usually the order parameter is defined as $\psi(\mathbf{r})=\phi(\mathbf{r})-\phi_c$, hence the deviation of the actual $\phi(\mathbf{r})$ from the mean value ϕ_c is formed. Inserting this definition into Eq. (2.1) shows that ϕ_c drops, leading to the thus defined correlation function [19].
[37] H. E. Stanley, *Introduction to Phase Transitions and Critical Phenomena* (Oxford University Press, Oxford, 1971).
[38] J. Zinn-Justin, Quantum Field Theory and Critical Phenomena (Oxford University Press, Oxford, 1989).
[39] H. Swinney and D. Henry, Phys. Rev. A **8**, 2586 (1973).
[40] M. Fixmann, J. Chem. Phys. **36**, 310 (1962).
[41] K. Kawasaki, Ann. Phys. (N.Y.) **61**, 1 (1970).
[42] T. A. Vilgis and G. Meier, J. Phys. I (France) **4**, 985 (1994).
[43] W. Theobald, A. Sans-Pennincks, G. Meier, and T. A. Vilgis (unpublished).
[44] H. C. Burstyn and J. V. Sengers, Phys. Rev. A **25**, 448 (1982).
[45] E. D. Siggia, B. I. Halperin, and P. C. Hohenberg, Phys. Rev. B **13**, 2110 (1976).
[46] H. C. Burstyn, J. V. Sengers, J. K. Bhattarcharjee, and R. A. Ferrell, Phys. Rev. A **28**, 1567 (1983).
[47] B. Momper, Ph.D. thesis, University of Mainz, Germany, 1989.
[48] T. M. Bender, R. J. Lewis, and R. Pecora, Macromolecules **19**, 244 (1986).
[49] V. G. Puglielli and N. C. Ford, Phys. Rev. Lett. **25**, 143 (1970).
[50] J. G. Shanks and J. V. Sengers, Phys. Rev. A **38**, 885 (1988).
[51] M. G. Brereton, E. W. Fischer, G. Fytas, and U. Murschall, J. Chem. Phys. **86**, 5174 (1987).
[52] V. L. Ginzburg, Fiz. Tverd. Tela (Leningrad) **x**, xxx (1960) [Sov. Phys. Solid State **2**, 1824 (1960)].
[53] P. G. de Gennes, J. Phys. Lett. **38**, 441 (1977).
[54] J. F. Joanny, J. Phys. A **11**, 117 (1978).
[55] F. J. Wegner, Phys. Rev. B **5**, 4529 (1972).
[56] M. E. Fisher and R. J. Burford, Phys. Rev. **156**, 583 (1967).
[57] D. Schwahn, L. Belkoura, and D. Woermann, Ber. Bunsenges. Phys. Chem. **90**, 339 (1986).
[58] L. D. Landau and E. M. Lifshitz, Fluid Mechanics (Pergamon, London, 1959).
[59] K. Perl and R. Ferrell, Phys. Rev. Lett. **29**, 51 (1972).
[60] M. Doi and A. Onuki, J. Phys. II (France) **2**, 1631 (1992).
[61] J. D. Ferry, *Viscoelastic Properties of Polymers* (Wiley, New Jersey 1980), Chap. 1.
[62] G. Meier, G. Fytas, B. Momper, and G. Fleischer, Macromolecules **26**, 5310 (1993).
[63] For a review, K. Binder and H. Sillescu, in *Encyclopedia of Polymer Science and Engineering* 2nd ed., edited by H. Mark *et al.* (Wiley, New Jersey, 1989).
[64] A. Z. Akcasu, G. Naegele, and R. Klein, Macromolecules **24**, 4408 (1991).
[65] M. Doi and S. F. Edwards, *The Theory of Polymer Dynamics* (Clarendon, Oxford, 1988), Chap. 5.
[66] J. V. Sengers, Int. J. Thermophys. **6**, 203 (1985).
[67] Q. H. Lao, B. Chu, and N. Kuwahara, J. Chem. Phys. **62**, 2039 (1975).
[68] K. Hamano, T. Nomura, T. Kawazura, and N. Kuwahara, Phys. Rev. A **26**, 1153 (1982).
[69] For example, C. Kappeler and L. Schäfer, Macromolecules **23**, 2766 (1990).